Contribution to the special issue of Physical Chemistry, Chemical Physics devoted to
"Interfacial Processes and Mechanisms",
in celebration of John Albery's 75th birthday.

Received 09 Nov 2010. Revised 12 Jan 2011. Accepted 18 Jan 2011

S. Fletcher and T.S. Varley,
Phys. Chem. Chem. Phys., 13, 5359-5364 (2011)

The institutional repository is at
http://dspace.lboro.ac.uk/dspace/handle/2134/8384

Published online first at **Phys. Chem. Chem. Phys., DOI: 10.1039/c0cp02471f.**

Beyond the Butler-Volmer Equation. Curved Tafel Slopes from Steady-State Current-Voltage Curves.

Stephen Fletcher and Thomas Stephen Varley

Department of Chemistry,
Loughborough University,
Ashby Road, Loughborough,
Leicestershire LE11 3TU, UK

Tel. 01509 22 2561 Fax 01509 22 3925
Email Stephen.Fletcher@Lboro.ac.uk

Keywords

Symmetry factor; Butler-Volmer Equation; Tafel Slope; Electron Transfer; Reaction Coordinate

Dedication

This article is part of the special collection on *Interfacial Processes and Mechanisms* in celebration of John Albery's 75th birthday.

Abstract

We report the discovery and analysis of curved Tafel slopes from the electrochemical reduction of hexamminecobalt(III) under steady-state conditions. In order to confirm the existence of the curvature, random assemblies of carbon microelectrodes (RAM™ electrodes) were employed to obtain experimental data over more than three orders of magnitude, without significant double layer charging currents and without ohmic distortion. Since the rate-determining step in the reduction reaction is electron transfer, and no ligand substitution reactions occur on the timescale of experiments, the curvature of the Tafel plot is attributed to the dependence of the symmetry factor on electrode potential.

Introduction

W. John Albery is the doyen of British electrochemists. The goal of his research over many years has been to understand the role of the electron in chemistry. In this regard his career provides an elegant counterpoint to that of his mentor, Ronald Percy Bell, who spent a lifetime elucidating the role of the proton in chemistry [**1**].

Early in his career, Albery advocated the use of the rotating disc electrode for the study of intermediates in electrode kinetics [**2**]. This helped establish a fourth great steady state technique in the electrochemist's repertoire (in addition to the dropping mercury electrode, the thin layer cell, and the microelectrode). Later, he helped develop electron transfer biosensors, and famously showed that it was possible to determine the free-energy profile of the redox reactions of cytochrome *c* at a surface-modified gold electrode [**3**]. In addition, he propelled conventional electrochemistry into the realm of unpaired electrons, and developed a novel tube electrode for performing electrochemical ESR [**4**]. Finally, among many other discoveries, Albery alerted the world to the importance of non-linear effects in both electrochemistry and in reactions in solution. The *locus classicus* is ref. [**5**].

One of the non-linear effects predicted by electron transfer theory is the curvature of Tafel slopes in systems where the electron transfer step is rate determining. Such a phenomenon is implied by the weak dependence of the symmetry factor on overpotential [**6-8**]. However, for more than fifty years, attempts to detect this curvature have been frustrated by the labyrinthine complexity of the experiments required. Typically, the accessible range of electrode potentials has proved too small, or the electrochemical rate constant has proved too large, to allow accurate conclusions to be drawn. Even in the few successful experiments reported in the literature (most notably ref. **6**), the difficulties have necessitated the use of non-steady state techniques. In the present work we report the first successful observation of a curved Tafel slope over a wide range of potentials under steady state conditions. This is made possible by the availability of large assemblies of microelectrodes and a redox couple that has a pathologically small rate constant.

Among the stringent criteria for observing curved Tafel slopes are:

i. A "slow" irreversible electron transfer step (no chemical rate-determining step, no back reaction)

ii. No ligand substitution in the inner sphere of the reactant species
iii. A single reactant species (no significant speciation)
iv. A high concentration of reactant species (no diffusion control)
v. A low faradaic background current (no parallel reactions)
vi. Minimal mains interference (or suitable digital filtering thereof)
vii. Minimal *IR* drop (minimal ohmic distortions)
viii. A high concentration of supporting electrolyte, and a low electrode potential (<1V) (no significant reactant adsorption)
ix. Minimal capacitive charging currents.
x. Enough data to provide 95% confidence in any derived parameter.

Failure to meet any of these criteria may lead to large errors in experimental results. In the literature, only Savéant and Tessier appear to have successfully negotiated the Thesean maze. They described and discussed data derived from the reduction of certain organic molecules, particularly nitro compounds, on mercury in acetonitrile and dimethylformamide containing tetrabutylammonium iodide as supporting electrolyte. The reduction of the nitro compounds gave rise to stable radical anions, which suggested that the overall mechanism was one of outer-sphere electron transfer. However, to counteract the effects of diffusion control, the authors found it necessary to use convolution potential sweep voltammetry, which is a technique for generating quasi-steady-state current-voltage curves from diffusion controlled cyclic voltammograms. Despite this complication, their study nevertheless established for the first time that the symmetry factor did indeed vary with electrode potential.

While not concerned with the symmetry factor *per se*, Bard and co-workers [**9, 10**] and Sun and co-workers [**11**] later carried out some ingenious measurements of electron transfer rates using scanning electrochemical microscopy. Among the advantages of the SECM technique are that (i) it operates in a steady-state, so contributions from capacitive charging are negligible; and (ii) it measures the faradaic current in a solution feedback mode, so background currents are minimized. By exploiting these properties, the authors were able to carry out measurements at the interface between two immiscible electrolyte solutions, where they observed an "inverted region" of electron transfer kinetics. The key data were obtained by fitting theoretical SECM approach curves to experimental approach curves at different applied potentials. Although the results were sparse, they were reproducible to within 10%, and so were considered reliable.

Not all authors, however, have been able to detect curved Tafel slopes, or inverted kinetics, despite strenuous efforts to do so. For example, Weaver and Anson measured the electrochemical reduction rates of three complexes of Cr(III) over a wide potential range, using a combination of chronocoulometry and dc polarography [**12**]. The three complexes studied, $[Cr(H_2O)_5SO_4]^+$, $[Cr(H_2O)_5F]^{2+}$, and $[Cr(H_2O)_6]^{3+}$ all supposedly followed outer-sphere electron transfer mechanisms, but even after applying diffuse double-layer corrections of various magnitudes the authors still could not observe any significant dependence of the symmetry factor on applied potential. The reason for this negative result remains a mystery.

More recently, the validity of Marcus theory for outer-sphere heterogeneous electron transfer reactions was critically examined by Clegg *et al*. [**13**]. These authors studied the oxidation of a series of anthracene derivatives in nitrile solvents. By contriving

steady-state conditions (by means of a high-speed channel electrode) the problem of charging currents was cleverly avoided. However, despite reporting highly precise measurements of exchange rate constants in a wide range of solvents, the authors did not comment on the existence, or otherwise, of curved Tafel slopes in the systems they studied. They did, however, demonstrate the advantages of steady state techniques when precise data were required.

The motivation for the present work was to measure curved Tafel slopes under steady-state conditions. In our case, we used random assemblies of carbon micro-discs (RAM™ electrodes) to record high-precision steady-state electron transfer rates over more than three orders of magnitude. The many and various design criteria for RAM™ electrodes have been summarized at length elsewhere [**14**], and will not be reproduced here. However, three features of RAM™ electrodes are worthy of special note. Firstly, they achieve steady-state diffusion-limited currents much faster than conventional macroelectrodes. The time t_{ss} taken to reach a steady-state current is proportional to the square of the radius of the individual micro-discs, since $t_{ss} \approx 400r^2/D$ where r is the radius of a micro-disc and D is the diffusion coefficient of the reactant. Hence, at RAM™ electrodes, steady-state currents can be recorded on the timescale of seconds without stirring the electrolyte solution. Secondly, RAM™ electrodes are much less sensitive to capacitively coupled mains interference than single microelectrodes. Thirdly, the micro-geometry of a RAM™ electrode generates an enhanced flux of reactant compared with a macroelectrode at the same potential, thus delaying the onset of diffusion control. In combination, these features significantly enhance the precision of Tafel slope measurements.

In order to compare our experimental results with electron transfer theory, it was important to make sure that the electron transfer step was rate determining (i.e. the electron transfer step was slower than any follow-up chemical reaction). Prior to beginning the present work, we therefore carefully searched the literature on homogeneous electron transfer reactions in order to find a redox couple that had a second order self-exchange rate constant below 10^{-4} $M^{-1}s^{-1}$. Of special interest was the hexamminecobalt(III)/(II) redox couple $[Co(NH_3)_6]^{3+/2+}$ which had earlier been thoroughly characterized by Hammershøi, Geselowitz and Taube [**15**] and shown to have an electron-self-exchange rate constant of $(3.9 \pm 1) \times 10^{-6}$ $M^{-1}s^{-1}$ at 40 °C and at an ionic strength of 2.5 M. This rate constant is about one billion times less than that of the well-known electron transfer mediator $[Ru(NH_3)_6]^{3+/2+}$ [**16**]. The reason for this exceptionally small rate constant is that electron transfer from high spin cobalt(II) to low spin cobalt(III) is symmetry forbidden. The hexamminecobalt(III)/(II) redox couple was also of interest because the speciation of cobalt ammine complexes had recently been determined by Ji *et al*. as a function of the concentration of free ammonia [**17**]. Their results indicated that essentially pure $[Co(NH_3)_6]^{3+}$ was present when the concentration of free ammonia exceeded 10^{-2} M. This was doubly convenient because an excess of ammonia in aqueous solution also strongly suppressed the non-specific adsorption of cobalt ammine complexes on carbon electrodes at negative potentials, due to the presence of excess ammonium ions;

$$NH_3 + H_2O = NH_4^+ + OH^-$$

For both these reasons, $[Co(NH_3)_6]^{3+}$ was an almost ideal target molecule for our studies.

Experimental

All chemicals were purchased from Sigma-Aldrich (Dorset, England) unless otherwise stated. The working electrode was a random assembly of *circa* 800 carbon fibre micro-disc electrodes (RAM™ electrode, CSIRO, Melbourne, Australia). The carbon micro-discs were the sectioned ends of conducting carbon fibres, 3.5 μm radius, embedded in epoxy resin. The area enclosing the micro-discs was 28 mm^2, and the median nearest-neighbour distance was 70 μm. In preparation for each experiment, the assembly was carefully cleaned to remove any adventitious adsorbates. Electrodes were polished in de-ionized water using 0.3 μm alumina powder (Alpha Alumina Powder, 600242, from Kemet, Marayong, Australia). Polished electrodes were then briefly rinsed in a 50/50 mixture of water and nitric acid (Fisher Scientific 70%, CAS 7697-37-2) before being briefly sonicated in pure water. The working solution was a mixture of 15 mL of 0.5 M ammonium chloride and 1 ml of ammonia solution (Fisher Scientific 35%, CAS 1336-21-6), which was then saturated with hexamminecobalt(III) chloride (~100 μM) prior to use. All water was obtained from a Millipore Milli-Q gradient A10 water filter (18.2 MΩ internal measurement), and all cell solutions were deoxygenated thoroughly before use.

Electrochemical data were obtained by using an ECO Chemie Autolab PGSTAT 20 potentiostat (Utrecht, The Netherlands), controlled by General Purpose Electrochemical System software (v4.9). No *IR* compensation or noise filters were applied at any stage during the data acquisition. Counter electrodes were fabricated in-house from Aldrich platinum gauze, 99.9%, 52 mesh (CAS 7440-06-4) and were machined into flags approximately 2 × 1 cm in size. The reference half cell was a saturated calomel electrode purchased from Spectronic Instruments, Leeds, UK.

The acquisition of high-precision steady-state voltammograms compelled certain experimental precautions. Scan rates were limited to values <20 mV s^{-1}. Voltammograms were also restricted to electrode potentials more positive than −0.6 V (*vs.* SCE) beyond which there was evidence of product precipitation in solution. To minimize interferences, Tafel plots were restricted to current values that were one order of magnitude greater than the background capacitive charging current (~1 nA), and one order of magnitude less than the diffusion limited current (~81 μA).

Theory

The theory of current-voltage curves lies at the heart of modern electrochemistry. The formulation used by most electrochemists derives from the classical work of John Alfred Valentine Butler, Tibor Erdey-Grúz and Max Volmer in the 1920's [**18, 19**]. For a single electron transfer reaction, this classical approach contains a dimensionless parameter, known as the symmetry factor, whose value is generally considered to be a weak function of electrode potential. In a recent paper, the Butler-Volmer equation was re-derived from quantum mechanical principles [**20**]. The derivation took place in two stages. First, Dirac's perturbation theory was used to solve the Schrödinger equation for electron transfer from one state to another. Second, current-voltage curves were obtained by integrating the single-state results over the full density of states in electrolyte solutions. Thermal equilibrium was assumed throughout. Somewhat surprisingly, it was found that the symmetry factor β_V that

appears in textbook derivations of the Butler-Volmer equation is different from the symmetry factor β_H that appears in modern electron transfer theory. The reason is clear from **Fig. 1.** Hereafter, to avoid ambiguity, we shall refer to these differently-defined symmetry factors as the *vertical symmetry factor* β_V and the *horizontal symmetry factor* β_H. We also note that the reactant and product parabolas may have slightly different curvatures, although we ignore that complication here.

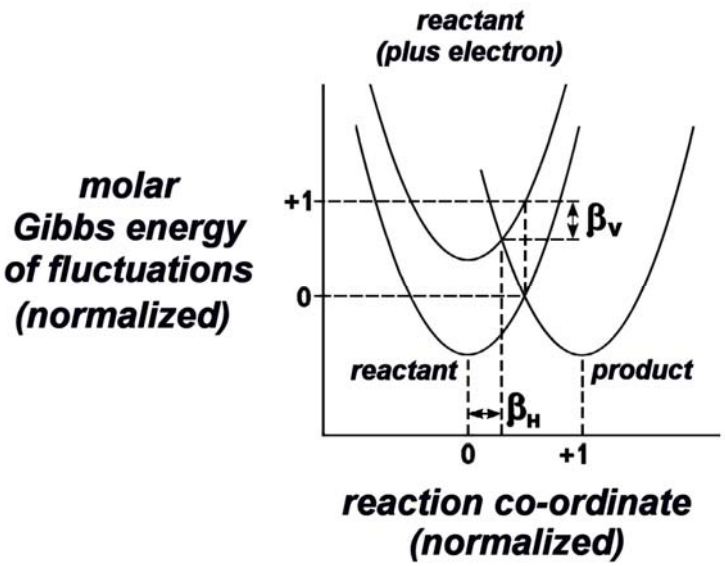

Fig. 1. Gibbs energy diagram for heterogeneous one-electron transfer from an electrode to a reactant in solution, in the normal regime of electron transfer, showing two different definitions of the symmetry factor. We call these the vertical symmetry factor β_V and the horizontal symmetry factor β_H.

In electrolyte solutions, electron transfer may take place in three possible regimes of driving force: the "inverted" regime (for reactions that are highly exergonic), the "normal" regime (for reactions that are almost in energy balance), and the "superverted" regime (for reactions that are highly endergonic) [21].

These regimes are defined as follows:

Inverted regime ($\Delta G_m^0 < -\lambda_m$).

Normal regime ($-\lambda_m < \Delta G_m^0 < \lambda_m$).

Superverted regime ($\Delta G_m^0 > \lambda_m$).

Here ΔG_m^0 is the molar Gibbs energy change of the reaction, and λ_m is the reorganization energy per mole. The *reorganization energy* may be thought of as the Gibbs energy that would hypothetically be required to replace the entire ionic atmosphere of the reactant species with the ionic atmosphere of the product species, in the absence of electron transfer. In the present work, we confine our attention to the "normal" regime of electron transfer, for a one-electron transfer process whose

reaction co-ordinate consists of a single quadratic degree of freedom (or a linear combination of multiple quadratic degrees of freedom).

For reactant and product parabolas of the same curvature it is readily found that:

$$\beta_H + ½ = 2\beta_V \qquad [1]$$

where, at positive overpotential in the "normal" regime, $0 \le \beta_H \le \frac{1}{2}$ and $\frac{1}{4} \le \beta_V \le \frac{1}{2}$.

Equation 1 shows that $\beta_H = \beta_V$ when both have the value ½. Since this is the value that is widely assumed in the literature, it perhaps explains why the difference between β_H and β_V has been widely ignored.

Explicitly, we may also write:

$$\beta_H = \frac{1}{2}\left(1 - \frac{F\eta}{\lambda_m}\right) \qquad [2]$$

and

$$\beta_V = \frac{1}{2}\left(1 - \frac{F\eta}{2\lambda_m}\right) \qquad [3]$$

where $F\eta$ is the molar Gibbs energy of electrons in the electrode and λ_m is the reorganization energy of the reactant species per mole. These equations suggest that the symmetry factor, howsoever defined, is a linear function of overpotential η.

Finally, in terms of the vertical symmetry factor β_V, the forward rate of electron transfer for a "slow" (rate-determining) one-electron transfer process may be written:

$$I = I_0 \exp\left(\frac{\beta_V F\eta}{RT}\right) \qquad [4]$$

Results

The experimental current-voltage curve for the cathodic reduction of ~100 μM $[Co(NH_3)_6]^{3+}$ at a random assembly of carbon micro-disc electrodes is shown in **Fig. 2.** These data were obtained at a scan rate of 10 mV s^{-1}. It is immediately clear that at potentials more negative than –0.6 V the reaction falls under diffusion control. In order to avoid confusion between this effect and genuine Tafel curvature, experimental data were truncated at –0.6 V, and at the same time Koutecký-Levich compensation for diffusion control was applied to the surviving data [22].

A typical result is shown in **Fig. 3.** The residual diffusion effect is slight, as revealed by the very slight divergence of the curves, but the effect of diffusion is still visible

above 8 μA, and so we decided to apply the Koutecký-Levich compensation routinely throughout the present work as a precautionary measure. This meant that we could be confident that any Tafel curvature remaining in our data after Koutecký-Levich compensation was NOT due to the onset of diffusion control.

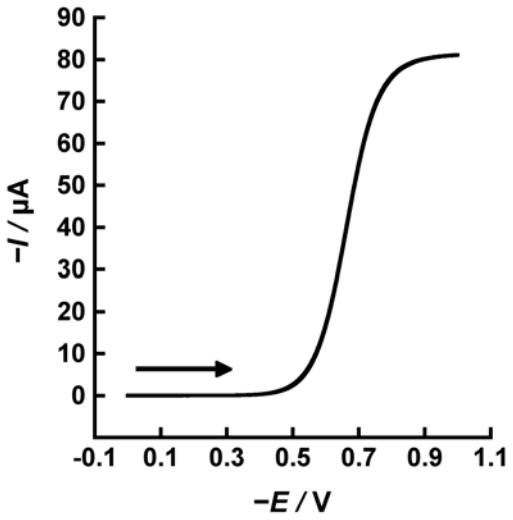

Fig. 2. Experimental current-voltage curve for the cathodic reduction of ~100 μM (aqueous) $[Co(NH_3)_6]^{3+}$ in a mixture of 15 mL of 0.5 M ammonium chloride and 1 ml of ammonia solution. The electrode was a random assembly of carbon micro-disc electrodes. Single scan at a scan rate of 10 mV s^{-1}. 3300 data points, 11-point moving average smoothing to filter capacitively-coupled mains interference (50 Hz).

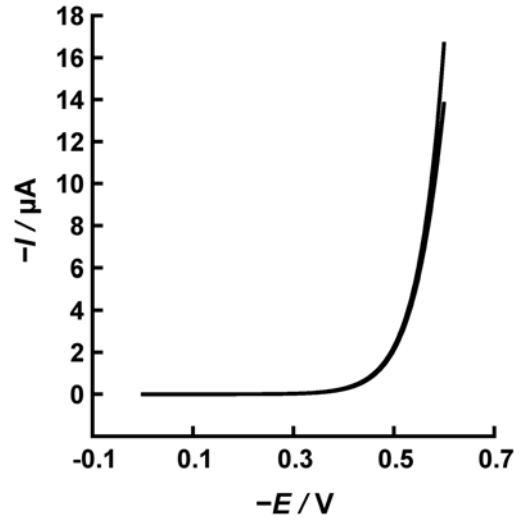

Fig. 3. Same data as Fig. 2, truncated at –0.6 V, showing the effect of Koutecký-Levich compensation. Top curve computed from bottom curve by multiplying by $[I_D/(I_D - I)]$, assuming I_D = 81 μA. 2000 data points, 11-point moving average smoothing to filter capacitively-coupled mains interference (50 Hz).

A classical Tafel plot for the cathodic reduction of ~100 μM $[Co(NH_3)_6]^{3+}$ at a random assembly of carbon micro-disc electrodes is shown in **Fig. 4**, using a scan rate of 10 mV s^{-1}, after Koutecký-Levich compensation. The plot is restricted to data that are one order of magnitude greater than the background capacitive charging current (~1 nA), and one order of magnitude less than the diffusion limited current (~81 μA).

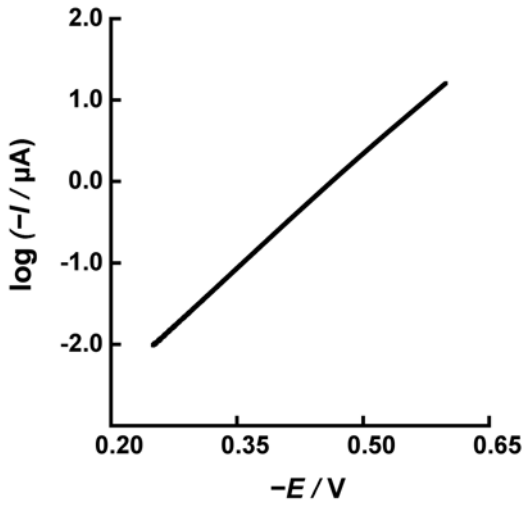

Fig. 4. Tafel plot for the cathodic reduction of ~100 μM $[Co(NH_3)_6]^{3+}$ at a random assembly of carbon micro-disc electrodes, including Koutecký-Levich compensation. Single scan at a scan rate of 10 mV s^{-1}. 2000 data points, 11-point moving average smoothing to filter capacitively-coupled mains interference (50 Hz).

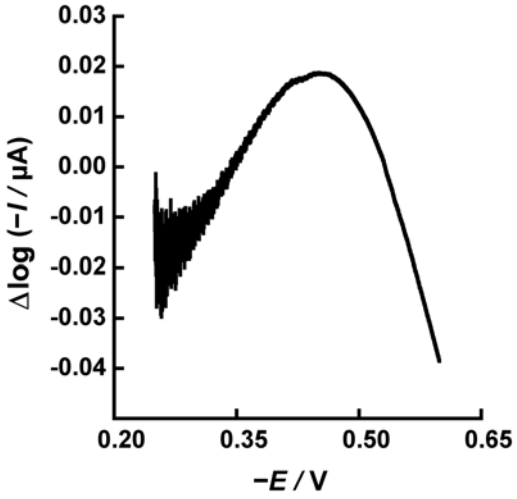

Fig. 5. Detection of curvature in the Tafel plot for the cathodic reduction of ~100 μM $[Co(NH_3)_6]^{3+}$ at a random assembly of carbon micro-disc electrodes. Error curve for the difference between experimental data and the linear line of best fit. An inverted parabolic shape is clearly evident. Residual mains interference is also prominent at low overpotentials (low currents).

The curvature of the plot is just visible to the naked eye, but it is more readily seen by plotting the error curve for the difference between the raw data and the linear line of best fit. When this transformation of the data is carried out, an inverted parabolic shape is readily observed, **Fig. 5.** This establishes that the experimental Tafel slope is indeed curved. Moreover, the effect is reproducible both within individual runs, and between different runs on different days.

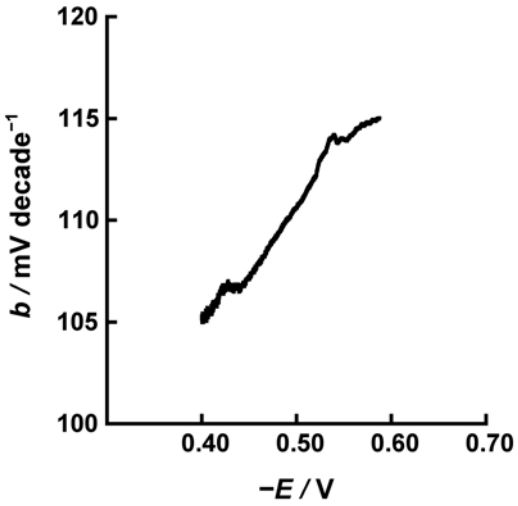

Fig. 6. Experimental variation of the Tafel slope, *b*, for the cathodic reduction of ~100 μM $[Co(NH_3)_6]^{3+}$ at a random assembly of carbon micro-disc electrodes. The small peaks are artefacts caused by a slight mismatch of the gains of the operational amplifiers used to record the data.

In an alternative representation, **Fig. 6** shows the first derivative of the experimental Tafel plot. This reveals how the Tafel slope, *b*, varies with applied potential. It can be seen that the Tafel slope varies from 105 mV decade^{-1} to 115 mV decade^{-1} over the experimentally-accessible range of overpotentials. Although this plot is sensitive to mains interference, the trend is clear.

Conclusions

Over the past century, slow progress in our understanding of interfacial electron transfer processes has gradually been made by a combination of kinetic, thermodynamic, and structural approaches. Nevertheless, the question of which factors determine the activation energy of electron transfer remains a contentious issue. A notorious problem has been the lack of reliable data regarding the reorganization energy per mole, λ_m. Applying the derivative of Eq. 3 to **Fig. 6** we estimate that, for the reduction of hexamminecobalt(III), $\lambda_m \approx 60$ kJ mol^{-1}. This is a large number, which not only explains why the curvature of the Tafel slope is so slight, but also lends credence to the idea that there may be substantial contributions to the reorganization energy from both "inner sphere" effects (mechanical fluctuations of bond lengths) and "outer sphere" effects (electrical fluctuations of charge

distribution). How the reorganization energy is partitioned between these different effects remains an open question, however. Nevertheless, from the present work, it may be concluded that some separation of the different effects might be achieved by extending the present experiments to cobalt complexes having different structures, and that remains an important challenge for the future.

Finally, it is interesting to compare the RAM™-derived Tafel slopes of hexamminecobalt(III), which undergoes "slow" electron transfer, with the RAM™-derived Tafel slopes of hexachloroiridate(III), hexacyanoferrate(III), and bis(η^5-cyclopentadienyl)iron(II) [Fc, ferrocene], which all undergo "fast" electron transfer **(Table 1).**

Table 1. Self-exchange rate constants for "fast" redox couples.

	k/ M^{-1} s^{-1}	μ/M	E^0/V	Ref.
$[IrCl_6]^{3+/2+}$ (aq)	2.3×10^5	0.10	0.89	23
$[Fe(CN_6)]^{3-/4-}$ (aq)	3.3×10^4	0.49	0.42	24
Fc/Fc^+ (acn)	7.5×10^6	0.15	—	25

The results are shown in **Figs. 7-9**. The experimental Tafel slopes are found to be 59.9, 61.7, and 63.5 mV decade^{-1}, respectively. These values are sufficiently close to the theoretical value for an EĈ reaction ($2.303RT/F \approx 59.2$ mV at 25°C) that we may be sure that, in each case, the interfacial electron transfer process is actually rate controlled by a chemical step. This implies that there is no curvature in the Tafel plots of these species caused by the potential dependence of the symmetry factor, and suggests that future attempts to find such curvature would be better directed towards species having Tafel slopes of ~118.4 mV decade^{-1}.

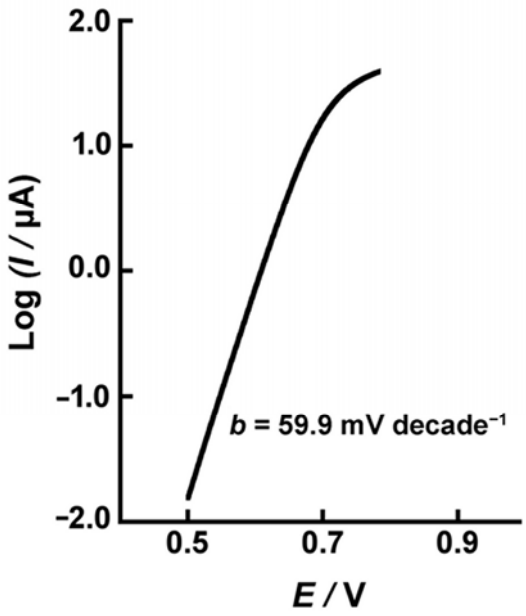

Fig. 7. Tafel plot for the anodic oxidation of 100 μM (aqueous) potassium hexachloroiridate(III) at a random assembly of carbon micro-disc electrodes (RAM™ electrode). The potential was held at 0.0 V *vs.* SCE for 10 s before scanning between 0.0 V and +1.0 V, at 20 mV s^{-1}.

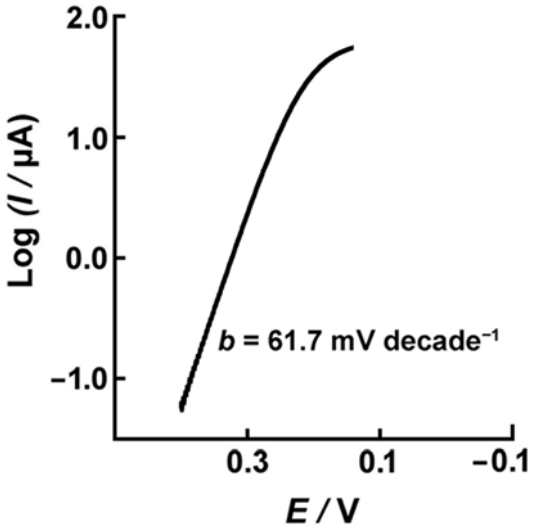

Fig. 8. Tafel plot for the cathodic reduction of 100 μM (aqueous) potassium hexacyanoferrate(III) at a random assembly of carbon micro-disc electrodes (RAM™ electrode). Supporting electrolyte was 0.5 M potassium nitrate. The potential was held at +0.8 V *vs*. SCE for 10 s before scanning between +0.8 V and −0.2 V, at 20 mV s^{-1}.

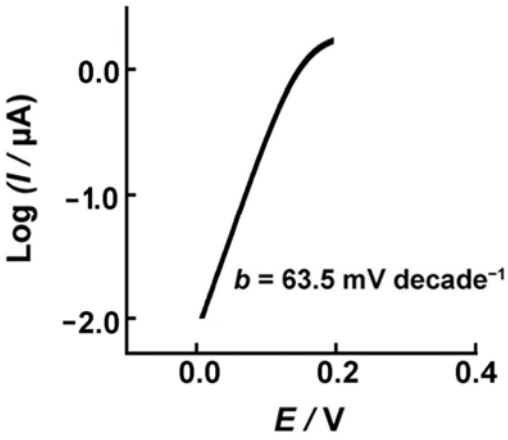

Fig. 9. Tafel plot for the anodic oxidation of 100 μM bis(η^5-cyclopentadienyl)iron(II) [ferrocene] in the ionic liquid butyltrimethylammonium bis(trifluoromethylsulfonyl) imide. Data recorded at a random assembly of carbon micro-disc electrodes (RAM™ electrode). The potential was held at −0.5 V *vs*. Ag/AgCl wire for 10 s before scanning between −0.5 V and +0.5 V, at 20 mV s^{-1}.

References

[1] R. P. Bell; "The Proton in Chemistry". Methuen & Co., London, (1959).

[2] W. J. Albery and M. L. Hitchman; "Ring-Disc Electrodes". Oxford: Clarendon Press, (1971).

[3] W. J. Albery, M. J. Eddowes, H. A. O. Hill and A. R. Hillman, J. Am. Chem. Soc., **103**, 3904-3910 (1981).

[4] W. J. Albery, B. A. Coles and A. M. Couper, Journal of Electroanalytical Chemistry, **65**, 901-909 (1975).

[5] W. J. Albery, Ann. Rev. Phys. Chem., **31**, 227-263 (1980).

[6] J-M. Savéant and D. Tessier, Faraday Discuss. Chem. Soc., **74,** 57-72 (1982).

[7] R. A. Marcus, J. Chem. Phys., **43**, 679-701 (1965).

[8] N. S. Hush, J. Chem. Phys., **28**, 962-972 (1958).

[9] S. Amemiya, Z. Ding, J. Zhou, A. J. Bard, J. Electroanal. Chem., **483**, 7-17 (2000).

[10] Z. Ding, B. M. Quinn, and A. J. Bard, J. Phys. Chem. B, **105**, 6367-6374 (2001).

[11] P. Sun, F. Li, Y. Chen, M. Zhang, Z. Zhang, Z. Gao and Y. Shao, J. Am. Chem. Soc., **125**, 9600-9601 (2003).

[12] M. J. Weaver and F. C. Anson, The Journal of Physical Chemistry, **80**, No. 17, 1861-1866 (1976).

[13] A. D. Clegg, N.V. Rees, O. V. Klymenko, B. A. Coles, and R. G. Compton, J. Am. Chem. Soc., **126**, 6185-6192 (2004).

[14] S. Fletcher and M.D. Horne, Electrochemistry Communications, **1**, 502-512 (1999).

[15] A. Hammershøi, D. Geselowitz and H. Taube, Inorganic Chemistry, **23**, 979-982 (1984).

[16] H. Taube, *Nonadiabatic Electron Transfer in Oxidation-Reduction Reactions*, Advances in Chemistry, **162**, Chapter 7, pp 127-144 (1977).

[17] X. Ji, F. G. Chevallier, A. D. Clegg, M. C. Buzzeo, and R. G. Compton, Journal of Electroanalytical Chemistry, **581**, 249-257 (2005).

[18] J. A. V. Butler, Trans. Faraday Soc., **19**, 729-733 (1924).

[19] T. Erdey-Grúz and M. Volmer, Z. Physik. Chem., **150**, 203-213 (1930).

[20] S. Fletcher, Journal of Solid State Electrochemistry, **13**, 537-549 (2009).

[21] S. Fletcher, Journal of Solid State Electrochemistry, **12**, 765-770 (2008).

[22] J. Koutecký and V. G. Levich, *The Application of the Rotating Disc Electrode to Studies of Kinetic and Catalytic Processes*, Zh. Fiz. Khim., **32**, 1565-1575 (1958).

[23] P. Hurwitz and K. Kustin, Trans. Faraday Soc., **62**, 427-432 (1966).

[24] H. Takagi and T.W. Swaddle, Inorg. Chem., **31**, 4669-4673 (1992).

[25] R. M. Nielson, G. E. McManis, L. K. Safford, and M. J. Weaver, J. Phys. Chem., **93**, 2152-2157 (1989).
